Journal of
Materials Chemistry B

Materials for biology and medicine

rsc.li/materials-b

Volume 6
Number 3
21 January 2018
Pages 341-528

ISSN 2050-750X

ROYAL SOCIETY
OF CHEMISTRY

PAPER
Wei Wei, Guanghui Ma et al
Macrophage responses to the physical burden of cell-sized particles

ROYAL SOCIETY
OF CHEMISTRY

rsc.li/materials-b

ARTICLE

MSC-Derived Osteogenic Cell Sheets on Stiffness-Tuned Hyaluronic Acid-Gelatin Hydrogels

Kelum Chamara Manoj Lakmal Elvitigala[a] and Shinji Sakai*[a]

Osteogenic cell sheets retain intercellular junctions and their native extracellular matrix, enabling stage-specific support for bone repair. To engineer such sheets under controlled mechanical cues, we developed stiffness-tuned composite hydrogels via enzymatic crosslinking of phenolated hyaluronic acid (HA-Ph) and gelatin (Gelatin-Ph) using horseradish peroxidase and hydrogen peroxide (H_2O_2). We evaluated the ability of these hydrogels to support osteogenic differentiation and enable cell sheet fabrication from human bone marrow-derived mesenchymal stem cells (bMSCs). Hydrogel stiffness was controlled by varying the degree of phenolation in HA-Ph (3.7, 4.3, and 5.2 phenol groups per 100 repeating units) at a fixed polymer concentration, resulting in hydrogels with Young's moduli of 3.3, 6.0, and 10.1 kPa, respectively. The stiffest hydrogel (10.1 kPa) enhanced YAP nuclear localisation in bMSCs, whereas the hydrogel with intermediate stiffness (6.0 kPa) most effectively induced osteogenic differentiation, as evidenced by the high expression levels of osteogenic marker genes, including ALP1, COL1A1, and RUNX2. By day 7, cells on the hydrogels had already initiated differentiation, enabling the detachment of cell sheets containing partially differentiated bMSCs, which were subsequently re-adhered to a new surface without losing their osteogenic potential. These findings demonstrate the potential of stiffness-tuned HA-Ph/Gelatin-Ph composite hydrogels as effective platforms for bone tissue engineering using cell sheets.

Introduction

Osteogenic cell sheets are emerging as powerful tools for bone tissue engineering owing to their ability to preserve cell-cell junctions and extracellular matrix (ECM) components, thereby providing stage-specific regenerative functions.[1] Early-stage sheets primarily exert paracrine effects that promote cell proliferation and angiogenesis, whereas mature sheets deposit mineralised matrices that directly support bone formation. Among possible cell sources, mesenchymal stem cells (MSCs) are particularly promising owing to their accessibility, multipotency, and well-documented osteogenic potential.[2] Therefore, MSC-derived osteogenic cell sheets offer a versatile platform for bone regeneration. However, to fully exploit their therapeutic potential, it is essential to design culture substrates that enable precise control over the differentiation stage at which sheets are harvested. Achieving such stage-specific outcomes requires culture substrates that deliver precise cues to direct cell fate. Hydrogels are suitable for this purpose because their mechanical properties can be tuned to regulate the mechanotransduction pathways that govern lineage commitment.[3,4] Prior studies have typically modulated hydrogel stiffness by altering polymer concentration or blend ratios.[5] Because polymer concentration significantly influences cellular responses, isolating mechanical cues requires maintaining a constant polymer concentration, while varying only the crosslink density. In this study, we modulated hydrogel stiffness

groups (e.g. via tyramine grafting) onto the alginate backbone enables enzyme-mediated oxidative coupling of phenols to form covalent dityrosine-like crosslinks[6]. At a fixed polymer concentration, increasing the degree of phenol substitution increases the crosslink density and mechanical properties of the resultant hydrogel. Carboxylate-containing polysaccharides are particularly suitable for this strategy: 1-Ethyl-3-(3-dimethylaminopropyl) carbodiimide (EDC)/N-hydroxysuccinimide (NHS) activation followed by coupling with amine phenols, introduces the required phenolic groups (-Ph). In this study, the same chemistry was applied to hyaluronic acid (HA), a carboxylate-rich ECM polymer, allowing grafting of phenol groups onto the HA backbone to achieve composition-invariant stiffness control.

We synthesised composite hydrogels from phenolated hyaluronic acid (HA-Ph) and phenolated gelatin (Gelatin-Ph), and enzymatically crosslinked them using horseradish peroxidase (HRP) and hydrogen peroxide (H_2O_2)[7]. Stiffness was adjusted by varying the number of phenol moieties on the HA backbone **(Fig. 1a)**, which changed the number of crosslinkable sites without altering the total polymer concentration. HA and gelatin, both major ECM components, possess unique properties that make them ideal for in vitro tissue engineering applications.[8,9] HA interacts with cell-surface receptors such as

a. Department of Materials Engineering Science, Graduate School of Engineering Science, The University of Osaka, Toyonaka, Osaka, 560-8531, Japan.
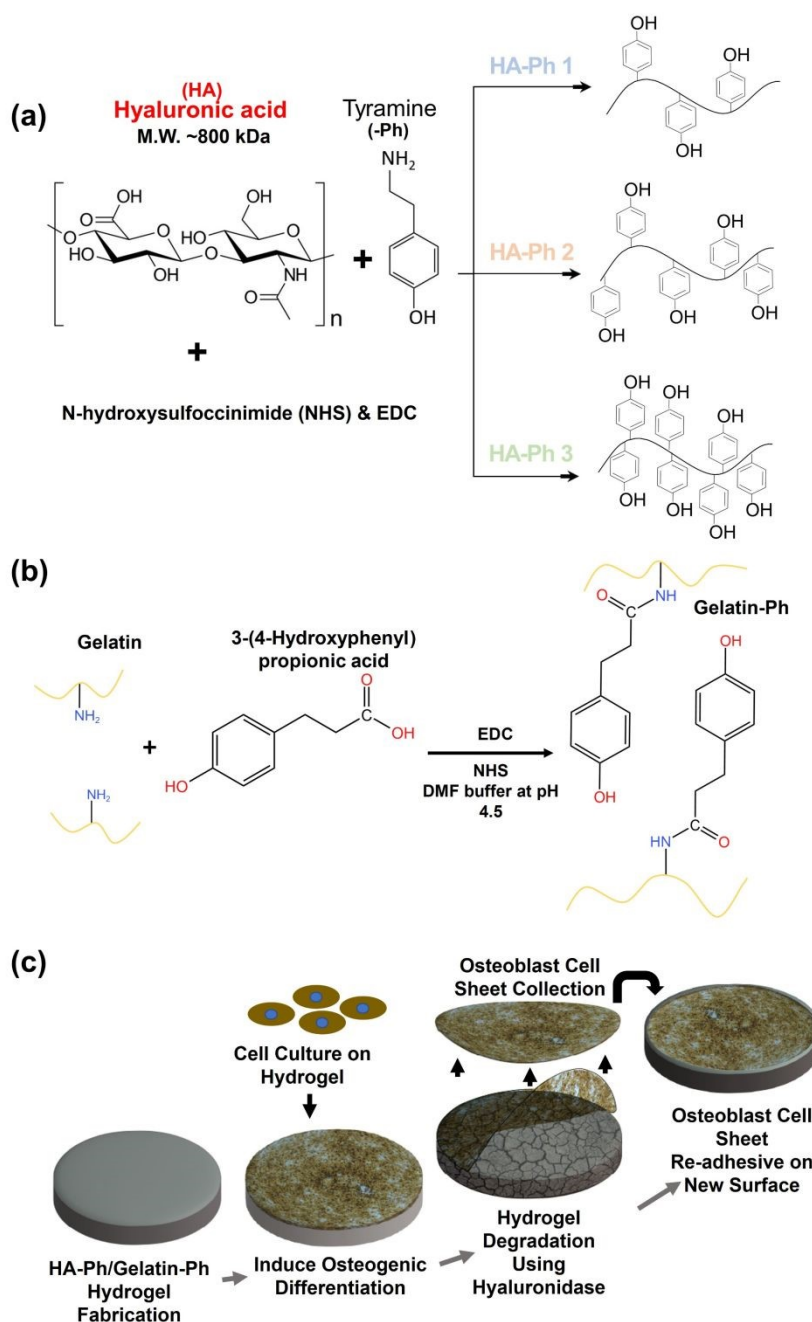*Corresponding author: sakai@cheng.es.osaka-u.ac.jp

Figure 1. Schematics of synthesis of phenolated (a) hyaluronic acid (HA-Ph) with varying amounts of phenol moieties introduced into the HA backbone and (b) gelatin (Gelatin-Ph). (c) Osteogenic cell sheet harvesting, in which the differentiated cell sheet is detached from the HA-Ph/Gelatin-Ph hydrogel via hyaluronidase treatment.

CD44 and RHAMM, playing crucial roles in osteogenesis and cell adhesion,[10,11] whereas gelatin, through its arginyl-glycyl-aspartic acid (RGD) peptides, facilitates integrin-mediated cellular signalling. Additionally, controlled degradation of the Gelatin-Ph/HA-Ph hydrogel by hyaluronidase allows cell sheet harvesting without the need for temperature control.[4]

Additionally, hydrogels with tuneable mechanical properties offer a versatile platform for modulating the cellular microenvironment via stiffness adjustments, which plays a crucial role in directing osteoblast functions, including differentiation via mechanotransduction pathways.[12] Several studies have demonstrated that stiff hydrogels promote osteogenic differentiation by enhancing the expression of osteogenic markers, such as RUNX2 and ALP1.[13] However, stiffness values of approximately 4–8 kPa have also been reported to support osteogenesis under specific conditions. This ability to fine-tune hydrogel stiffness enables control over the extent of osteoblast differentiation, offering a valuable tool

for bone tissue engineering. In the context of cell sheet fabrication, stiffness-tuneable hydrogels can be employed to generate cell sheets with varying degrees of differentiation. These differentiated cell sheets can potentially be used at different stages of bone repair or in other regenerative medicine applications, offering a versatile platform for clinical use.

We hypothesised that HA-Ph/Gelatin-Ph hydrogels with tuneable stiffness can regulate the osteogenic differentiation of human bone marrow-derived mesenchymal stem cells (bMSCs) and enable the fabrication of cell sheets at defined stages of differentiation via hyaluronidase-mediated enzymatic detachment **(Fig. 1b)**. Hyaluronidase selectively cleaves the HA-Ph component, releasing intact sheets while preserving cell viability and deposited matrix. Accordingly, we evaluated cell adhesion, osteogenic differentiation, and sheet formation across hydrogels with defined Young's moduli to establish a stiffness-optimised platform capable of harvesting early, intermediate, and more mature osteogenic sheets.

Materials and Methods

Materials

HA-Ph with 3.7, 4.3, and 5.2 phenol groups per 100 repeating units (referred to as HA-Ph 3.7, HA-Ph 4.3, and HA-Ph 5.2, respectively) and Gelatin-Ph (4.1×10^{-4} mol-Ph/g) were synthesised according to previously reported protocols (the detailed procedures are provided in ESI), and phenol contents were determined based on the tyramine standard curve **(Fig. S1b)**.[14] Sodium hyaluronate (HA-LQ; average molecular weight, 550 kDa) was purchased from Kewpie (Tokyo, Japan). Tyramine hydrochloride was purchased from Chem-Impex (IL, USA). 3-(4-Hydroxyphenyl)propionic acid was obtained from Tokyo Chemical Industry (Tokyo, Japan). Type B gelatin (bovine skin) was obtained from Sigma-Aldrich (MO, USA). Phalloidin-iFluor 488 (ab15.2759) was purchased from Abcam (Cambridge, UK). N-Hydroxysulfoccinimide, 3-ethylcarbodiimide hydrochloride, 4% paraformaldehyde, hyaluronidase, catalase from bovine liver, HRP, 31% w/w hydrogen peroxide (H_2O_2) aqueous solution, and phosphate-buffered saline (PBS) containing 4% w/w paraformaldehyde were purchased from FUJIFILM Wako Pure Chemical (Osaka, Japan).

Cell culture

The human bone marrow-derived mesenchymal stem cell line UE7T-13, immortalised with HPV E7 and hTERT, was obtained from RIKEN BioResource Center (Ibaraki, Japan). Cells were cultured at 37 °C in a humidified incubator with 5% CO_2 using Dulbecco's modified Eagle's medium (DMEM) (Peptide Institute, Osaka, Japan) supplemented with 10% v/v fetal bovine serum (FBS).

Gelatin-Ph and HA-Ph characterisation

The phenol moieties introduced into HA were quantified via UV-Vis spectrophotometry (UV-2600, Shimadzu, Kyoto, Japan) based on absorbance at 275 nm. [1]H nuclear magnetic resonance (NMR) spectroscopy (JNM ECS-400, JEOL, Tokyo, Japan) was performed to confirm the incorporation of phenol moieties into the HA backbone **(Fig. S2-3)**.

Gelation time and diphenol formation analysis

A 1 mL PBS solution containing 2% w/v HA-Ph (HA-Ph 3.7, HA-Ph 4.3, or HA-Ph 5.2), 0.5% w/v Gelatin-Ph, and 50 U/mL HRP was poured into a well of a 12-well plate and exposed to air containing 16 ppm H_2O_2 under stirring for gelation time measurements. Gelation time was defined as the time required to form a dome-shaped hydrogel around the magnetic stir bar. Diphenol formation was analysed utilising a fluorescence plate reader (Molecular Devices, San Jose, CA, USA). The polymer solution (100 μL) was added to a 96-well plate, and fluorescence emission between 350 and 600 nm was measured at an excitation wavelength of 310 nm. The peak at approximately 420 nm indicated diphenol formation.

Enzymatic degradation

The enzymatic degradability of the HA-Ph/Gelatin-Ph hydrogels was evaluated using three types of HA-Ph with different phenol substitution degrees. Hydrogels were prepared by enzymatic crosslinking of 2% w/v HA-Ph, 0.5% w/v Gelatin-Ph, and 50 U/mL HRP, followed by exposure to air containing 16 ppm H_2O_2 for 30 min. Hydrogels (8 mm in diameter and 2 mm in height) were fabricated for each HA-Ph variant and subsequently immersed in 1 mL of DMEM containing 0.1% w/v hyaluronidase at 37 °C. Morphological changes were monitored over a 4-h period **(Fig. S4)**.

Scanning electron microscopy (SEM) observation of freeze-dried hydrogels

Specimens for SEM observation were prepared using a freeze-extraction method. A precursor solution consisting of 2% w/v HA-Ph, 0.5% w/v Gelatin-Ph, and 50 U/mL HRP in 1 mL of PBS was poured into a polydimethylsiloxane (PDMS) mould (8 mm diameter, 4 mm height), and exposed to air containing 16 ppm H_2O_2 for 30 min. The formed hydrogels were then frozen at −80 °C and subsequently immersed in 70% ethanol followed by 100% ethanol at −30 °C for a total of 10 h to extract water while preserving the internal structure. The dehydrated specimens were vacuum-dried, and the cross-sections were sputter-coated with a thin layer of gold prior to imaging. Microstructures were observed using a field-emission scanning electron microscope (SEM; JCM-6000plus, JEOL, Tokyo, Japan) operated at an acceleration voltage of 15 kV.

Swelling ratio analysis

HA-Ph/Gelatin-Ph hydrogels were prepared under the same preparation conditions used for the enzymatic degradation study. The hydrogels were first lyophilised to obtain their dry weight (W_dry) and subsequently immersed in PBS at 37 °C for swelling analysis **(Fig. S5)**. At predetermined time intervals, the samples were removed from PBS, gently blotted to remove excess surface moisture, and weighed to obtain the swollen

ARTICLE

weight (W_swollen). The swelling ratio was calculated as the relative increase in mass compared with the dry state, using the equation Q = (W_swollen – W_dry) / W_dry. All measurements were conducted in triplicate for each HA-Ph variant.

Hydrogel preparation for cell culture

Hydrogels were prepared in a 6-well plate by pouring PBS containing HA-Ph (2.0% w/v), Gelatin-Ph (0.5% w/v), and HRP (50 U/mL), followed by exposure to air containing 16 ppm H_2O_2 for 30 min. The stiffness of each hydrogel was measured using a material tester (EZ-SX; Shimadzu, Kyoto, Japan) equipped with an 8 mm probe. The hydrogels were compressed at 6 mm/min, and the Young's modulus was calculated from the stress–strain curve at 1–10% strain at 37 °C.

Cell adhesion and Yes-associated protein (YAP) localisation analysis

Hydrogels were prepared as described in the 'Hydrogel preparation for cell culture' section. Prior to cell seeding, DMEM with catalase (0.1% w/v) was added to the hydrogels and incubated overnight to degrade unreacted H_2O_2. Cells (5 × 10^3/cm²) were seeded onto each hydrogel and cultured for 2 days. The cells were then fixed with 4% paraformaldehyde for 30 min at 25 °C before staining. Following fixation, the cells were immersed in 0.1% Triton X-100 for 10 min to enhance permeabilisation, followed by incubation in 5% BSA to block non-specific antibody binding. Subsequently, cells were incubated overnight at 4°C with a fluorescence-conjugated (488) primary antibody targeting YAP (1:500 dilution in blocking buffer). The cells were stained with phalloidin-iFluor 647 (Abcam, Cambridge, UK) for F-actin and with DAPI for the nuclei. The stained cells were imaged utilising a fluorescence microscope (APX100; Olympus, Tokyo, Japan). The aspect ratio and YAP/TAZ localisation were analysed using ImageJ software (version 2.1.0/1.53c, NIH, Bethesda, MD, USA).

Osteoblast differentiation

Cells (5 × 10^4/cm²) were seeded onto the hydrogel and cultured in growth medium (DMEM) for 2 days. Upon reaching confluence, the growth medium was replaced with osteogenic differentiation medium (PT-3002; Lonza, Basel, Switzerland), and the cells were cultured for 21 days.

Alizarin Red S and alkaline phosphatase staining for osteoblast

After 21 days of osteogenic induction, cells were washed with PBS and fixed with 4% (w/v) paraformaldehyde for 30 min. For Alizarin Red S (Wako, Osaka, Japan) and ALP staining, fixed cells were washed with Milli-Q water and incubated for 30 min in 2 v/v% Alizarin Red S solution. After washing with MilliQ water, the cells were imaged utilising a fluorescence microscope (APX-100, Olympus, Tokyo, Japan) in the bright-field mode. For ALP activity quantification, cell lysates were prepared using 0.1 v/v% Triton X-100 in 50 mM 2-amino-2-methyl-1-propanol (AMP) buffer at 4 °C, followed by centrifugation (12,000×g, 10 min, 4 °C). Enzymatic activity was measured by incubating the lysates

with p-nitrophenyl phosphate (pNPP) substrate in AMP buffer at 37 °C for 30 min. The reaction product, p-nitrophenol, was quantified by measuring the absorbance at 405 nm employing a spectrometer (Molecular Devices, San Jose, CA, USA).

Quantitative real time polymerase chain reaction (qRT-PCR) analysis

Cells were collected from the hydrogel by incubation in growth medium containing hyaluronidase (1 mg/mL). Quantitative real-time polymerase chain reaction (qRT-PCR) was performed to assess the expression of RUNX2 (Runt-related transcription factor 2), COL1A1 (collagen type I alpha 1 chain), and alkaline phosphatase (ALP1). Total RNA was extracted using an RNA isolation kit (Takara, Shiga, Japan) and reverse transcribed into cDNA utilising a reverse transcription kit (Takara). qRT-PCR was performed using the TB Green Premix Ex Taq II kit (Takara) on a Thermal Cycler Dice Real Time System III (Takara Bio) Real-Time PCR System. Each reaction contained 10 ng of cDNA, 10 µL of TB Green master mix, and 0.4 µM of each forward and reverse primer in a total volume of 20 µL. The cycling conditions were as follows: initial denaturation at 95 °C for 30 s, followed by 40 cycles of 95 °C for 5 s and 60 °C for 30 s, with subsequent melt-curve analysis to confirm single-peak amplification. GAPDH was used as the internal reference gene. Primer sequences are presented in **Table S1**. All experiments were performed in duplicate, and gene expression levels were quantified employing the comparative Ct (-ΔΔCt) method**.

Cell sheet fabrication

Cells were cultured on the hydrogel in an osteogenic differentiation medium for 7 days. The medium was replaced with a growth medium containing hyaluronidase (1 mg/mL) and incubated for 10 min to detach the cell sheets from the hydrogel surface. After an additional 15 min of incubation, the detached cell sheets were collected using a pipette and transferred to a fresh well plate. The re-adhesiveness of the cell sheets in the well plate was assessed using a light microscope after 1 day of post-culture, after which the growth medium was replaced with differentiation medium. Differentiation of the cell sheets was confirmed via Alizarin Red S staining, as mentioned in the previous section, after 21 days of culture.

Statistical analysis

Data analysis was performed using Microsoft Excel 2019 version 1808 (Microsoft Corp., Redmond, WA, USA). One-way analysis of variance (ANOVA) was used for statistical analyses, followed by Tukey's HSD post-hoc t-test. Differences were considered statistically significant at $p < 0.05$.

Results and Discussion

Characterisation of composite hydrogel

The properties of the HA-Ph/Gelatin-Ph hydrogels were analysed, including gelation time, Young's modulus, diphenol formation, and enzymatic degradation, swelling ratio, alongside
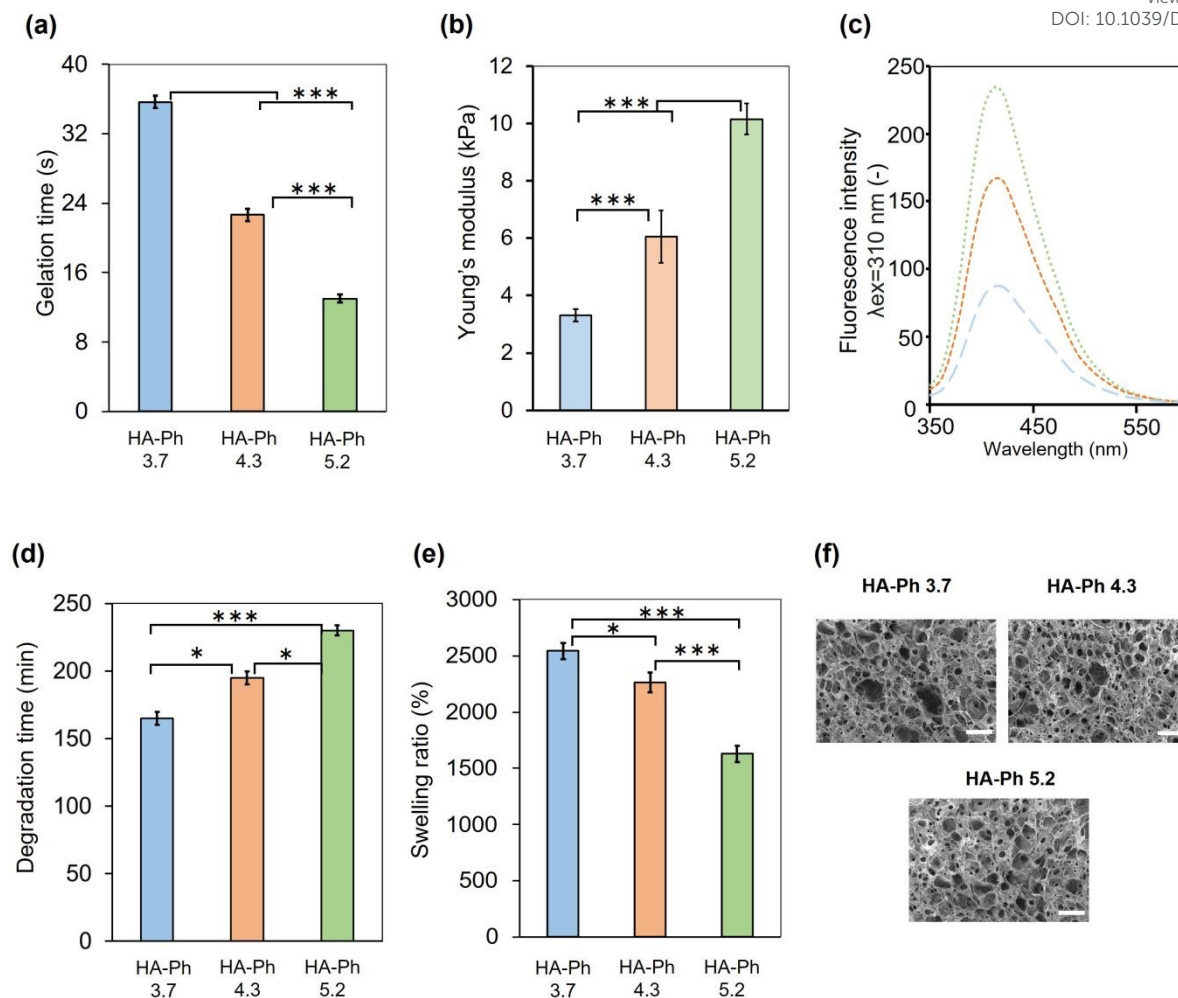
Figure 2. Effect of phenol moiety content on the HA backbone on the physicochemical properties of HA-Ph/Gelatin-Ph hydrogels. (a) Gelation time, (b) Young's modulus, (c) fluorescence emission spectra with an excitation wavelength of 310 nm, (d) enzymatic degradation using 0.1% w/v hyaluronidase, and (e) swelling ratio of the hydrogel prepared with different degrees of phenol substitution. (f) Scanning electron microscopy images of cross-sections of freeze-dried Gelatin-Ph/HA-Ph hydrogels (scale bar: 500 μm). Error bars represent standard deviation (n = 3–5). $^*p < 0.05$, $^{***}p < 0.005$, Tukey HSD.

SEM-based structural characterisation (**Fig. 2**). Regarding gelation time, the 2% w/v HA-Ph and 0.5% w/v Gelatin-Ph polymer solution containing HA-Ph 3.7 exhibited the longest gelation time (36 s), whereas the HA-Ph 4.3 containing polymer solution gelled 33% faster, and the HA-Ph 5.2 solution, with the highest phenol content, gelled 64% faster, reaching 13 s (**Fig. 2a**). Young's modulus measurements, calculated from stress–strain curves between 1–10% strain (**Fig. S3**), indicated that the hydrogel prepared with HA-Ph 3.7 exhibited the lowest Young's modulus (3.3 kPa), approximately 45% and 67.3% lower than those of hydrogels containing HA-Ph 4.3 (6.0 kPa) and HA-Ph 5.2 (10.1 kPa), respectively (**Fig. 2b**). To further verify the crosslinking density, diphenol formation was assessed as an indirect measure of the degree of crosslinking. The HA-Ph/Gelatin-Ph hydrogel prepared using the solution containing HA-Ph 3.7 exhibited the lowest fluorescence intensity, followed by the hydrogel prepared using HA-Ph 4.3, whereas the HA-Ph 5.2 hydrogel exhibited the highest fluorescence emission at 420 nm (**Fig. 2c**). These results demonstrate a clear relationship

between the phenol content (-Ph) of HA-Ph and the resulting hydrogel properties, where an increased -Ph content resulted in faster gelation, higher stiffness, and higher crosslinking density. The observed trends align with previous studies showing that higher -Ph content enhances crosslinking, thereby reducing gelation time and increasing Young's modulus via the formation of a denser polymer network.[15] Similar trends in crosslinking enhancement via phenol modification have also been reported in HA-based hydrogel systems, confirming the role of phenol groups in tuning mechanical properties and gelation kinetics.[16] Enzymatic degradation of the hydrogels was also evaluated using hyaluronidase to assess the influence of phenol content on network stability. The degradation time increased with increasing phenol substitution, consistent with the formation of a denser and more tightly crosslinked network. Hydrogels prepared with HA-Ph 3.7 exhibited the shortest degradation time (165 min), whereas hydrogels containing HA-Ph 4.3 required a longer degradation time (195 min). The HA-Ph 5.2 hydrogels, which possessed the highest crosslinking density,

showed the slowest degradation, requiring 230 min to fully degrade under hyaluronidase exposure **(Fig. 2d)**. These results demonstrate that increasing phenol content enhances enzymatic resistance, reflecting the greater crosslink density of the hydrogels. The swelling behaviour of the hydrogels also showed a clear dependence on the phenol substitution degree. Hydrogels prepared with HA-Ph 3.7 exhibited the highest swelling ratio, absorbing approximately 1.5-fold more water than those prepared with HA-Ph 5.2. The HA-Ph 4.3 hydrogels showed an intermediate swelling ratio, which was ~11% lower than HA-Ph 3.7 and ~39% higher than HA-Ph 5.2 **(Fig. 2e)**. This trend indicates that increased phenol content, which promotes higher crosslinking density, restricts water uptake and results in reduced swelling capacity. These observations are consistent with the expected behaviour of phenol-mediated enzymatically crosslinked networks, in which tighter polymer networks limit hydrogel expansion.

Fig. 2f shows the cross-sectional SEM images of the freeze-dried hydrogels prepared using HA-Ph 3.7, HA-Ph 4.3, and HA-Ph 5.2. No significant difference in pore size or internal porous architecture was observed among the three hydrogel variants, despite their different phenol substitution degrees. This suggests that the variations in phenol content, while producing clear differences in mechanical properties, swelling ratios, and enzymatic degradation behaviour, did not induce substantial changes in ice nucleation or ice crystal growth during the freeze-extraction process. As the porous structures of freeze-dried hydrogels are primarily governed by the dynamics of ice formation during freezing rather than by moderate differences in crosslink density, it is reasonable that all three hydrogels exhibited similar pore morphologies. These observations align with previous reports indicating that the freeze-drying microstructure is largely dictated by ice nucleation and crystal growth kinetics, whereas the influence of polymer crosslinking is comparatively minor under identical freezing conditions.

Cellular adhesiveness and YAP/TAZ localisation

Understanding the influence of substrate mechanics on cell morphology is essential because osteoblast behaviour is strongly regulated by the physical properties of the extracellular environment. The aspect ratio, defined as the ratio of cell length
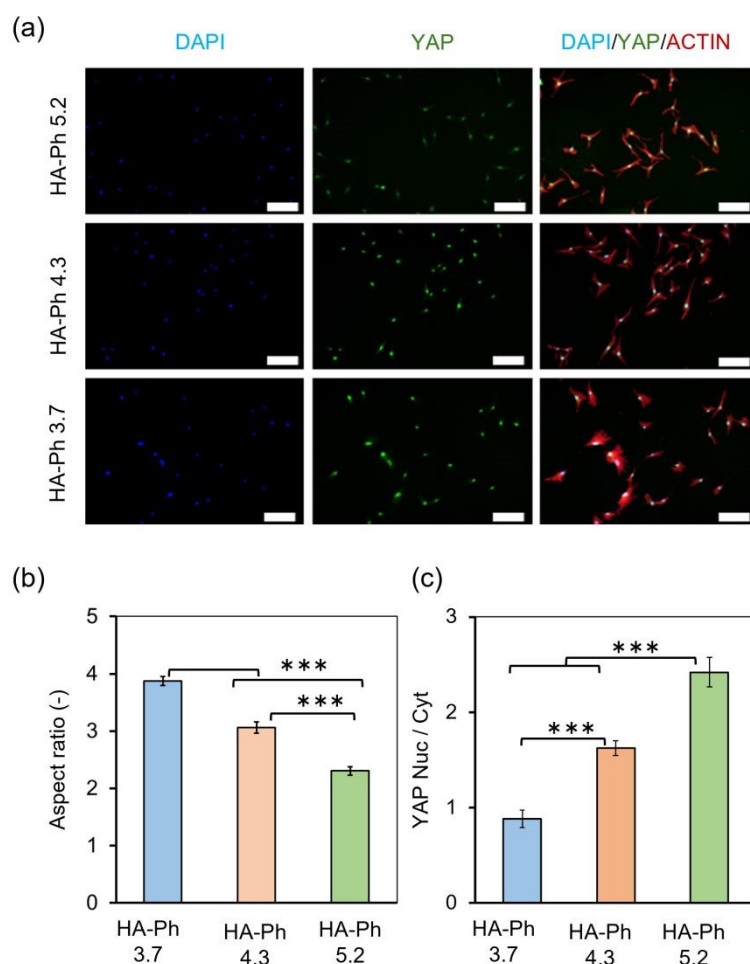

Figure 3. YAP localisation and cell morphology of UE7T-13 cells cultured on HA-Ph/Gelatin-Ph hydrogels. (a) Representative immunofluorescence images showing DAPI-stained nuclei (blue), YAP (green), and F-actin (red) of cells cultured on hydrogels prepared with HA-Ph 3.7, HA-Ph 4.3, and HA-Ph 5.2. Effect of hydrogel stiffness on (b) cell aspect ratio and (c) nuclear-to-cytoplasmic (Nuc/Cyt) ratio of YAP. Bar: standard deviation (n = 3). ***p < 0.005, Tukey HSD. Scale bars: 100 μm.

ARTICLE

to width, serves as a key indicator of cell elongation and is closely associated with mechanotransduction and osteogenic commitment. As shown in **Fig. 3,** the aspect ratio of cells decreased as hydrogel stiffness increased. Cells cultured on the HA-Ph/Gelatin-Ph hydrogel prepared using solutions containing HA-Ph 3.7 (3.3 kPa) and HA-Ph 4.3 (6 kPa) exhibited elongated morphologies, with aspect ratios of 3.8 and 3.0, respectively (**Fig. 3a, b**). By contrast, cells on the stiffest hydrogel containing HA-Ph 5.2 (10.1 kPa) showed a 39% reduction in aspect ratio compared with those on the HA-Ph 3.7 hydrogel, despite its higher stiffness. Several previous studies have also demonstrated that substrate rigidity significantly influences cell morphology; for example, Engler et al. showed that an intermediate stiffness (around 5 kPa) supports optimal cytoskeletal organisation and cell elongation, whereas substrates that are too stiff (approximately 10 kPa) tend to restrict cell spreading due to increased resistance and altered focal adhesion dynamics.[17] The higher phenol (-Ph) content in the HA-Ph/Gelatin-Ph hydrogel prepared with HA-Ph 5.2 may further enhance cell adhesion via biochemical interactions.[18]

To assess mechanotransduction, we analysed the Yes-associated protein (YAP) nuclear localisation, a key transcriptional regulator in stiffness-dependent signalling (**Fig. 3a, c**). The nuclear-to-cytoplasmic (Nuc/Cyt) YAP ratio increased with increasing hydrogel stiffness (**Fig. 3c**). Specifically, cells cultured on the softest hydrogel (HA-Ph 3.7, 3 kPa) exhibited a Nuc/Cyt ratio of 0.9, which increased to 1.6 on the HA-Ph 4.3 (6 kPa) containing hydrogel and reached 2.4 on the stiffest hydrogel (HA-Ph 5.2, 10 kPa). Such results are consistent with previous studies showing that stiffer substrates enhance YAP nuclear translocation, reinforcing its role in osteoblast cellular functions. For example, Dupont et al. demonstrated that increased matrix stiffness drives YAP/TAZ nuclear localisation, which in turn activates transcriptional programs that promote cell proliferation and osteogenic differentiation.[19,20]

Differentiation analysis

Given that cytoskeletal tension and mechanotransduction are critical for osteogenesis, we evaluated the osteogenic differentiation of UE7T-13 cells cultured on HA-Ph/Gelatin-Ph hydrogels containing different HA-Ph variants (HA-Ph 3.7, HA-Ph 4.3, and HA-Ph 5.2) for 21 days. Alizarin Red S and ALP staining were used to confirm differentiation, revealing significant differences in mineralisation and ALP activity across the stiffness range (**Fig. 4a, b**). The hydrogel with intermediate stiffness (HA-Ph 4.3, 6.0 kPa) promoted the highest degree of osteogenic differentiation, whereas both the softer (HA-Ph 3.7; 3.3 kPa) and stiffer (HA-Ph 5.2; 10.1 kPa) hydrogels exhibited comparatively reduced Alizarin Red S and ALP staining. Quantitative analysis of ALP enzymatic activity further substantiated these observations, with the highest absorbance at 405 nm observed in cells cultured on the HA-Ph 4.3 hydrogel (0.67), followed by HA-Ph 3.7 (0.29) and HA-Ph 5.2 (0.28) (**Fig. 4c**).
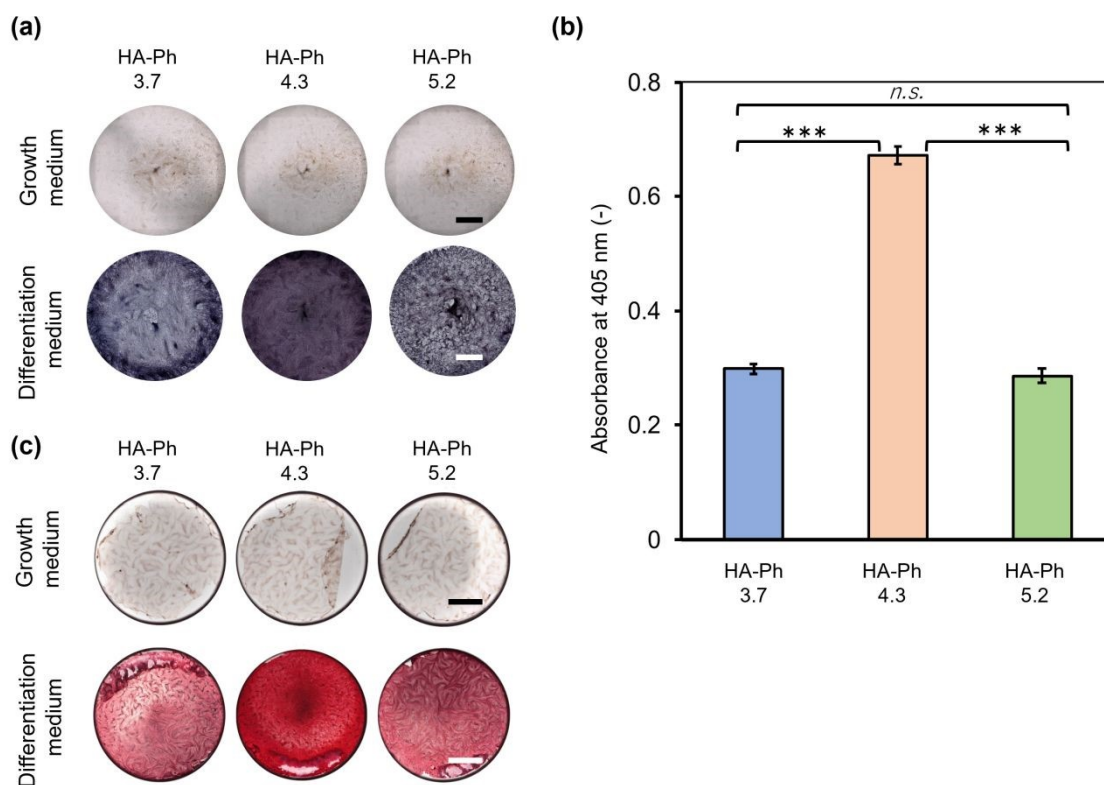

Figure 4. Effect of hydrogel stiffness on the osteogenic differentiation of UE7T-13 cells. (a) Alkaline phosphatase (ALP) staining of cells after 21 days of culture and (b) Quantification of ALP absorbance in cell lysates. (c) Alizarin Red S staining of cells after 21 days of culture. Bar: standard deviation (n = 3). Scale bars: 200 μm. ***p < 0.005, *n.s.*: p > 0.05 Tukey HSD.

ARTICLE

Journal Name

The stiffest hydrogel (HA-Ph 5.2) suppressed osteogenic differentiation, despite promoting strong cell adhesion and nuclear localisation of YAP, as shown previously. We hypothesised that the high concentration of phenol moieties in this hydrogel, despite being mechanically advantageous, may introduce biochemical cues that interfere with osteogenic signalling.[19] This suggests that biochemical cues can override mechanical signals; although stiffness enhances YAP translocation, excessive phenol groups may counteract this differentiation. Therefore, the interplay between mechanical and biochemical cues is critical, with the intermediate stiffness of the HA-Ph 4.3 hydrogel providing an optimal balance for osteogenic differentiation. The stiffness-dependent increase in YAP nuclear localisation observed in our study is also consistent with the mechanotransduction model reported by Dupont et al.[19] Furthermore, previous work on phenol-modified HA hydrogels by Sakai et al. supports our findings that increasing phenol content enhances crosslinking density and stiffness.[21] Notably, the highest stiffness did not elicit the strongest biological response in our system. This non-linear behaviour is consistent with general mechanobiology studies demonstrating that cellular functions do not necessarily increase monotonically with stiffness, and that matrix mechanics, matrix tethering, and surface chemistry jointly regulate cell activity.[22] Additionally, literature on matrix surface chemistry (e.g., Trappmann et al.) suggests that biochemical cues such as phenol density may also influence protein adsorption and cell fate, supporting our interpretation that both mechanical and biochemical factors contribute to the observed biological outcomes.[23]

qPCR analysis

To elucidate the molecular mechanisms underlying stiffness-dependent osteogenic differentiation, quantitative real-time PCR

(qPCR) analysis was performed. The genes selected for RUNX2, COL1A1, and ALP1 are critical markers representing key stages of osteoblast differentiation. RUNX2 acts as a master transcription factor that initiates osteogenesis, COL1A1 encodes type I collagen, the primary extracellular matrix protein in bone, and ALP1 encodes alkaline phosphatase, an early marker of mineralisation. Evaluating the expression of these genes provides insights into how substrate stiffness regulates osteogenic differentiation at the transcriptional level. Gene expression was assessed using qPCR after 7 days of osteogenic induction. GAPDH was selected as the reference gene following stability evaluation of multiple housekeeping genes. The hydrogel with intermediate stiffness (HA-Ph 4.3; 6.0 kPa) exhibited the highest expression of all three genes **(Fig. 5)**. Specifically, RUNX2 expression on the HA-Ph 4.3 hydrogel was 1.5-fold higher than that on the softest hydrogel (HA-Ph 3.7). Similarly, COL1A1 expression, associated with extracellular matrix production, was the highest in HA-Ph 4.3 (1.89), followed by HA-Ph 3.7 (1.14), with HA-Ph 5.2 (0.87) showing the lowest expression. The expression of ALP1, a marker of early osteoblast differentiation, followed the same trend, showing the highest expression in HA-Ph 4.3 (1.59), reinforcing that this stiffness range optimally supports osteogenic differentiation (**Fig. 5**). These transcriptional data strongly corroborate the protein-level findings from ALP staining and activity assays, confirming that an intermediate stiffness of ~6 kPa provides an optimal microenvironment for osteogenic differentiation. Our findings that substrate stiffness modulates the expression of osteogenic markers align with previous reports. For example, Khatiwala et al. demonstrated that stiffer extracellular matrices enhance ERK signalling and subsequently upregulate RUNX2 expression, a critical transcription factor driving osteogenesis.[24] Similarly, Gao et al. confirmed that mechanical cues from a stiffer bone microenvironment promote osteogenic differentiation in preosteoblasts, as evidenced by higher ALP activity and increased collagen type I expression.[25] Conversely, Yuan et al. discussed the broader influence of substrate stiffness in
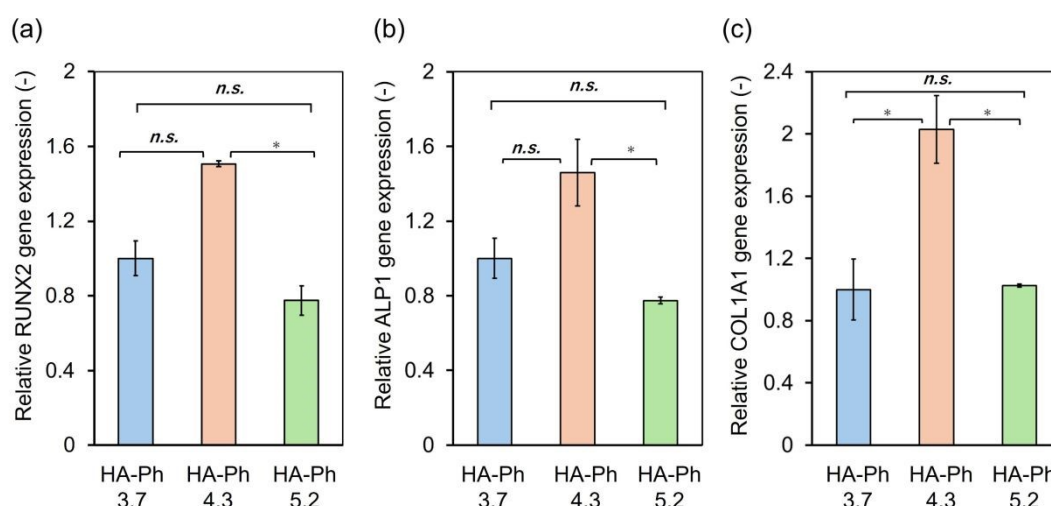

Figure 5. qPCR analysis of osteogenic marker gene expression in UE7T-13 cells cultured on HA-Ph hydrogels. Relative mRNA expression levels of (a) RUNX2, (b) ALP1, and (c) COL1A1 after 7 days of differentiation on HA-Ph 3.7, HA-Ph 4.3, and HA-Ph 5.2 hydrogels. Gene expression was normalised to GAPDH using the 2-ΔΔCt method. Bar: standard deviation (n = 3). $^*p$ < 0.05, n.s.: p > 0.05 Tukey HSD.

regulating cell behaviour, however, the connection to increased expression of osteogenic markers such as COL1A1 and ALP1 was not directly supported by their findings.[26] Instead, they focused more broadly on the molecular mechanisms of regulation. Collectively, these studies support the notion that substrate stiffness is a key biomechanical cue that activates signalling pathways, leading to increased RUNX2 and ALP1 expression, which in turn enhances osteogenic differentiation.

Cell sheet fabrication

To evaluate the potential of HA-Ph/Gelatin-Ph hydrogels for cell sheet fabrication, UE7T-13 cells were cultured on these hydrogels for 7 days to form partially differentiated cell sheets, which were subsequently harvested via enzymatic degradation using hyaluronidase (1 mg/mL). Prior to detachment, phase-contrast imaging validated that the cells formed continuous and confluent layers on all the hydrogel formulations (**Fig. 6**). Following enzymatic degradation of the hydrogel, the cell sheets were successfully detached while maintaining their structural integrity. The harvested sheets were readily transferred to a new culture plate, where they re-adhered within a few hours. After an additional 14 days of culture in the

colonies, and undergo osteogenic differentiation.[27] Similarly, studies on thermoresponsive microgel films have shown that harvested cell sheets exhibit robust adhesion properties and functional integrity, although detailed quantification of structural integrity was not provided.[28] Therefore, enzymatic degradation represents an effective alternative method for cell sheet recovery, achieving outcomes similar to conventional thermoresponsive approaches.

Limitations and future perspectives

Although this study provides compelling evidence for the influence of hydrogel stiffness and surface hydrophobicity on the regulation of osteoblast differentiation and cell sheet fabrication, several limitations must be addressed to facilitate its clinical application.

First, our evaluations were conducted in vitro using UE7T-13 cells to assess adhesion, morphology, and osteogenic differentiation on stiffness-tuned hydrogels. Although these results demonstrate clear trends, in vitro systems cannot fully replicate the complex physiological conditions of living tissues, such as immune responses, vascularisation, and mechanical loading. In particular, the fabricated osteoblast cell sheets were
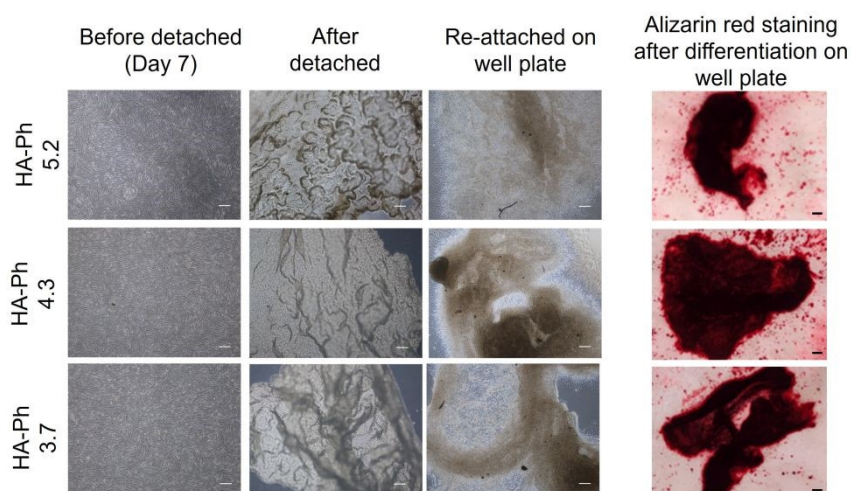

Figure 6. Osteogenic differentiation of UE7T-13 cells on HA-Ph/Gelatin-Ph hydrogels, cell sheet detachment, and differentiation. (a) Inverted optical microscopy images of UE7T-13 cells cultured on HA-Ph 3.7, HA-Ph 4.3, and HA-Ph 5.2 hydrogels before detachment. (b) Images of detached cell sheets obtained following enzymatic degradation of the hydrogel. (c) Reattached cell sheets on a new culture surface. (d) Alizarin Red S staining of reattached cell sheets after 14 days of culture. Scale bars: 100 μm.

differentiation medium, Alizarin Red S staining confirmed that the transferred cell sheets retained a strong mineralisation potential.

These results demonstrate that the HA-Ph/Gelatin-Ph hydrogel supports the formation, gentle detachment, and sustained osteogenic function of cell sheets, highlighting its suitability for bone tissue engineering applications. Prior studies have demonstrated that cell sheets obtained from the enzymatic degradation of hydrogels exhibit re-adhesiveness and retain essential cellular functions.[4] For instance, Yan et al. demonstrated that cells released from enzymatically controlled chitosan hydrogels maintained their ability to reattach, form

only tested for re-adhesion and differentiation on new culture substrates, without validation in biological environments. Therefore, future studies must investigate their integration, stability, and bone regeneration efficacy at the defect sites in in vivo models. Second, although this study focused on osteogenic differentiation, UE7T-13 cells possess multipotent characteristics and may differentiate into other mesenchymal lineages, such as chondrocytes or adipocytes, depending on environmental cues. The present experimental design does not exclude the possibility that stiffness or surface properties may direct differentiation toward other bone-related or mesenchymal cell types. Additional studies using lineage-specific markers or broader transcriptomic profiling may

provide valuable insights to confirm lineage commitment. Finally, although hydrogel stiffness was systematically varied and analysed, surface hydrophobicity—which is also known to influence cell behaviour—was not independently controlled in this study. Disentangling the effects of stiffness and surface hydrophobicity is crucial for achieving a deeper mechanistic understanding.

Conclusions

This study highlights the significant role of hydrogel stiffness and phenol content in modulating osteoblast differentiation and cell sheet fabrication using HA-Ph/Gelatin-Ph hydrogels. Our findings demonstrate that an intermediate stiffness (HA-Ph 4.3, 6 kPa) provides an optimal environment for osteogenic differentiation, as evidenced by the elevated expression levels of osteogenic markers (ALP1, COL1A1, and RUNX2) and enhanced mineralisation. By contrast, stiffer hydrogels (HA-Ph 5.2, ~10.1 kPa) promoted enhanced cellular adhesion and increased YAP nuclear translocation; however, their surface chemistry appeared to suppress osteogenic differentiation. These results suggest that hydrogel stiffness is not the sole determinant of differentiation; instead, the interplay between the mechanical properties and biochemical factors, such as surface chemistry, plays a significant role in regulating cell behaviour. Furthermore, the successful fabrication of partially differentiated osteoblast cell sheets from these hydrogels, their non-disrupting cell-cell interactions, and their subsequent reattachment and continued differentiation on new substrates highlight the potential of this hydrogel system for bone tissue engineering. The tuneable stiffness and controllable degradation of the HA-Ph/Gelatin-Ph composite hydrogels provide a versatile and promising platform for cell sheet engineering and broader regenerative medicine applications.

Author Contributions

K. C. M. L. E.: Conceptualization, Methodology, Investigation, Data Curation, Formal Analysis, Writing – Original Draft, Writing – Review & Editing, Visualization. S. S.: Conceptualization, Methodology, Resources, Funding Acquisition, Writing – Original Draft, Writing – Review & Editing, Supervision. All authors have given approval for the final version of the manuscript.

Conflicts of interest

There are no conflicts to declare.

Data availability

All experimental data within the article and supplementary information are available from the corresponding author upon reasonable request.

References

1   D. Ma, L. Ren, Y. Liu, F. Chen, J. Zhang, Z. Xue and T. Mao, *J. Orthop. Res.*, 2010, **28**, 697–702.
2   M. F. Pittenger, A. M. Mackay, S. C. Beck, R. K. Jaiswal, R. Douglas, J. D. Mosca, M. A. Moorman, D. W. Simonetti, S. Craig and D. R. Marshak, *Science (80-.).*, 1999, **284**, 143–147.
3   K. Chamara, M. Lakmal Elvitigala, L. Mohan, W. Mubarok, S. Sakai, K. C. M. L. Elvitigala, W. Mubarok, S. Sakai and L. Mohan, *Adv. Healthc. Mater.*, 2024, 2303787.
4   K. C. M. L. Elvitigala, W. Mubarok and S. Sakai, *Soft Matter*, 2023, **19**, 5880–5887.
5   E. Ferchichi, S. Stealey, P. Bogert and S. P. Zustiak, *Front. Biomater. Sci.*, 2024, **3**, 1408748.
6   S. Sakai and K. Kawakami, *Acta Biomater.*, 2007, **3**, 495–501.
7   K. C. M. L. Elvitigala, W. Mubarok and S. Sakai, *Biomolecules*, DOI:10.3390/BIOM14050604.
8   G. Camci-Unal, D. Cuttica, N. Annabi, D. Demarchi and A. Khademhosseini, *Biomacromolecules*, 2013, **14**, 1085–1092.
9   M. Rezaeeyazdi, T. Colombani, A. Memic and S. A. Bencherif, *Mater. 2018, Vol. 11, Page 1374*, 2018, **11**, 1374.
10 T. Ooki and M. Hatakeyama, *BioEssays*, 2020, **42**, 2000005.
11 M. Kawano, W. Ariyoshi, K. Iwanaga, T. Okinaga, M. Habu, I. Yoshioka, K. Tominaga and T. Nishihara, *Biochem. Biophys. Res. Commun.*, 2011, **405**, 575–580.
12 T. Luo, B. Tan, L. Zhu, Y. Wang and J. Liao, *Front. Bioeng. Biotechnol.*, 2022, **10**, 817391.
13 W. Zhao, X. Li, X. Liu, N. Zhang and X. Wen, *Mater. Sci. Eng. C. Mater. Biol. Appl.*, 2014, **40**, 316–323.
14 S. Bagheri, Z. Bagher, S. Hassanzadeh, S. Simorgh, S. K. Kamrava, V. T. Nooshabadi, R. Shabani, M. Jalessi and M. Khanmohammadi, *J. Biomed. Mater. Res. Part A*, 2021, **109**, 649–658.
15 F. F. Karageorgos and C. Kiparissides, *Int. J. Mol. Sci. 2021, Vol. 22, Page 7317*, 2021, **22**, 7317.
16 W. Wang, Z. Sun, Y. Xiao, M. Wang, J. Wang and C. Guo, *Acta Biomater.*, 2024, **187**, 138–148.
17 C. M. Lo, H. B. Wang, M. Dembo and Y. L. Wang, *Biophys. J.*, 2000, **79**, 144–152.
18 S. Sakai, K. Hirose, K. Moriyama and K. Kawakami, *Acta Biomater.*, 2010, **6**, 1446–1452.
19 S. Dupont, L. Morsut, M. Aragona, E. Enzo, S. Giulitti, M. Cordenonsi, F. Zanconato, J. Le Digabel, M. Forcato, S. Bicciato, N. Elvassore and S. Piccolo, *Nature*, 2011, **474**, 179–184.

20   S. Piccolo, S. Dupont and M. Cordenonsi, *Physiol. Rev.*, 2014, **94**, 1287–1312.

21   S. Sakai and M. Nakahata, *Chem. – An Asian J.*, 2017, **12**, 3098–3109.

22   A. Buxboim, J. Irianto, J. Swift, A. Athirasala, J. W. Shin, F. Rehfeldt and D. E. Discher, *Mol. Biol. Cell*, 2017, **28**, 3333.

23   B. Trappmann, J. E. Gautrot, J. T. Connelly, D. G. T. Strange, Y. Li, M. L. Oyen, M. A. Cohen Stuart, H. Boehm, B. Li, V. Vogel, J. P. Spatz, F. M. Watt and W. T. S. Huck, *Nat. Mater.*, 2012, **11**, 642–649.

24   C. B. Khatiwala, P. D. Kim, S. R. Peyton and A. J. Putnam, *J. Bone Miner. Res.*, 2009, **24**, 886–898.

25   S. Gao, B. Chen, M. Gao, Y. Xu, X. Yang, C. Yang and S. Pan, *Biomimetics 2023, Vol. 8, Page 344*, 2023, **8**, 344.

26   H. Yuan, Y. Zhou, M. S. Lee, Y. Zhang and W. J. Li, *Acta Biomater.*, 2016, **42**, 247–257.

27   X. Z. Yan, A. W. G. Nijhuis, J. J. J. P. Van Den Beucken, S. K. Both, J. A. Jansen, S. C. G. Leeuwenburgh and F. Yang, *Macromol. Biosci.*, 2014, **14**, 1004–1014.

28   Y. Xia, X. He, M. Cao, C. Chen, H. Xu, F. Pan and J. R. Lu, *Biomacromolecules*, 2013, **14**, 3615–3625.

Data availability

All experimental data within the article and supplementary information are available from the corresponding author upon reasonable request.